

高温溶体化処理したAl-6Si-4Cu合金鋳物のポアと疲労特性の関係

稲森, 隆晃
豊橋技術科学大学大学院機械工学系

戸田, 裕之
豊橋技術科学大学機械工学系

小林, 正和
豊橋技術科学大学機械工学系

中澤, 満
慶應大学理工学部

他

<https://hdl.handle.net/2324/1812246>

出版情報 : Journal of Japan Foundry Engineering Society. 85 (2), pp.69-75, 2013-02-01. Japan Foundry Engineering Society

バージョン :

権利関係 :

Table 1 The conditions of solution and aging treatments.

No.	Solution treatment	Aging treatment
1	807K for 3.6ks	443K for 18.0ks
2	807K for 10.8ks	443K for 18.0ks
3	773K for 36.0ks	443K for 18.0ks

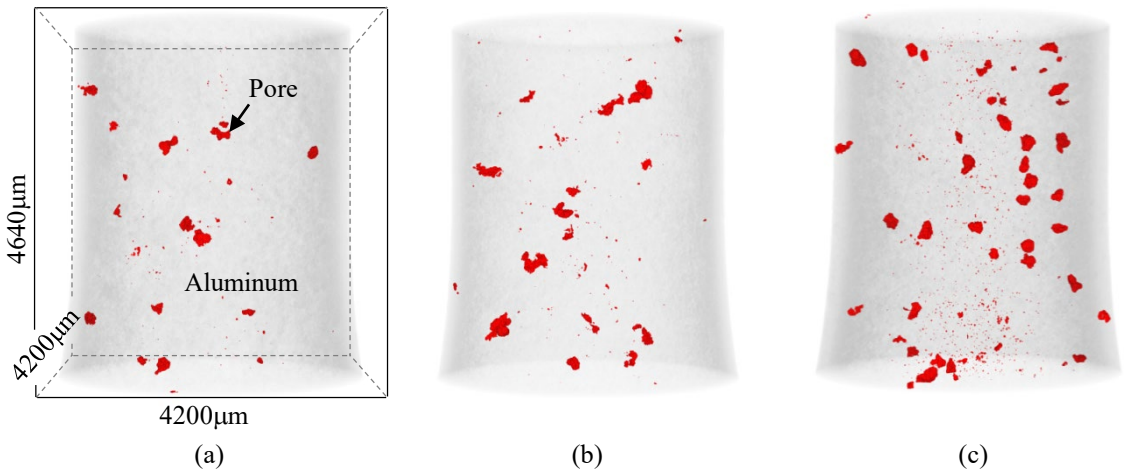


Fig.1 Typical 3D rendered perspective views of tomographic data, representing the distribution of pores in the materials that had been solution-treated at (a) 807K for 3.6ks ($V_f = 0.044\%$), (b) 807K for 10.8ks ($V_f = 0.072\%$) and (c) 773K for 36.0ks ($V_f = 0.111\%$). V_f is volume fraction of pores.

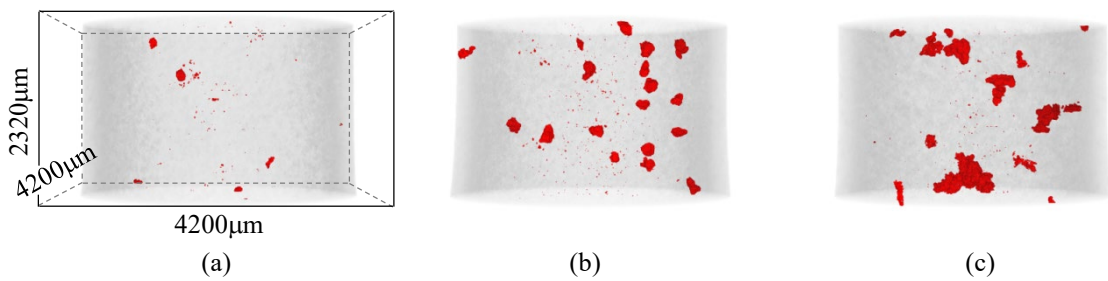


Fig.2 3D rendered perspective views of tomographic data, representing the distribution of pores in the three different specimens that had been solution-treated at 773K for 36.0ks.(a) $V_f = 0.019\%$, (b) $V_f = 0.111\%$, (c) $V_f = 0.323\%$.

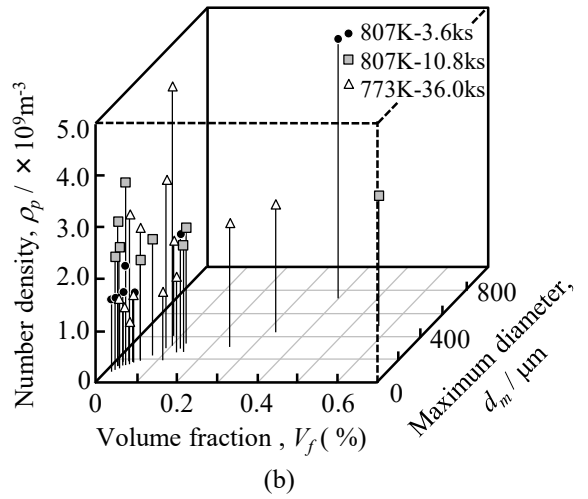
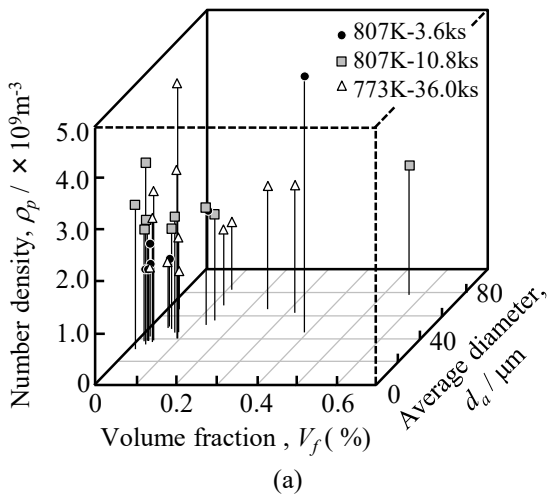


Fig.3 Results of quantitative analysis representing relationships among volume fraction, number density and diameter of what;(a)average diameter and (b)maximum diameter.

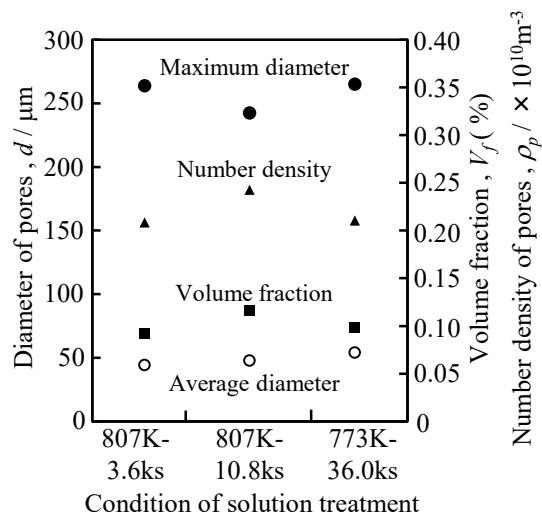


Fig.4 Results of quantitative analysis on various morphological parameters in each condition.

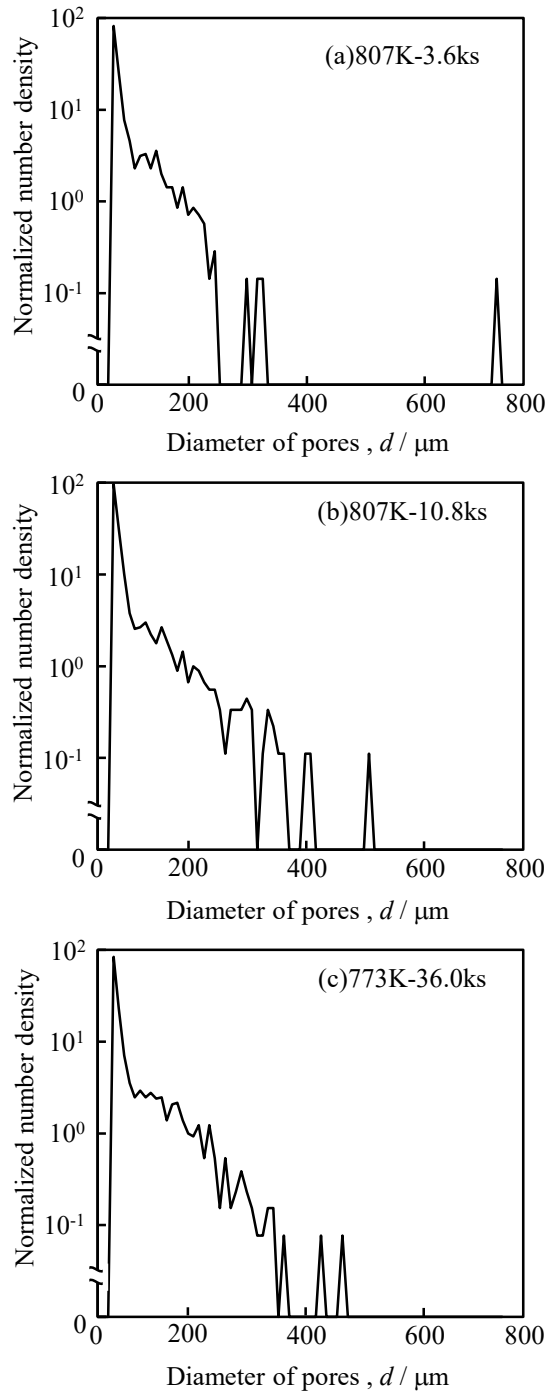


Fig.5 Histogram of normalized number density of pores at all specimens that after (a)807K for 3.6ks (b)807K for 10.8ks (c)773K for 36.0ks solution treatment.

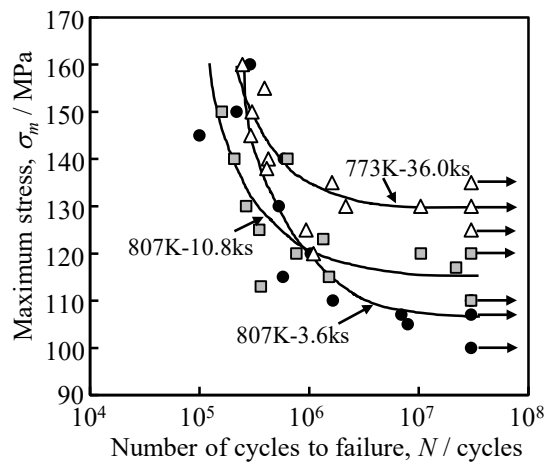


Fig.6 S-N curves in the fatigue tests .

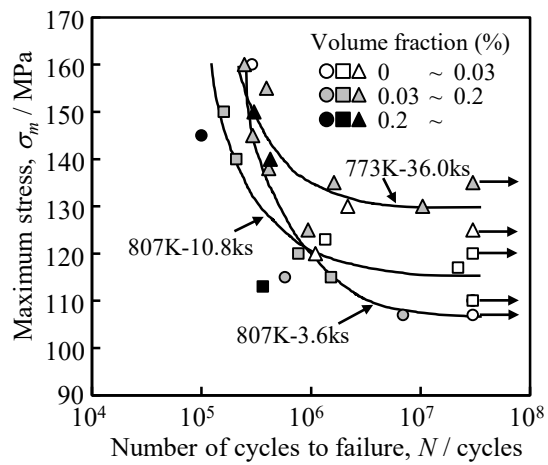


Fig.7 Classification of the data points shown in the S-N plots of Fig.6 according to the level of volume fraction of pores.

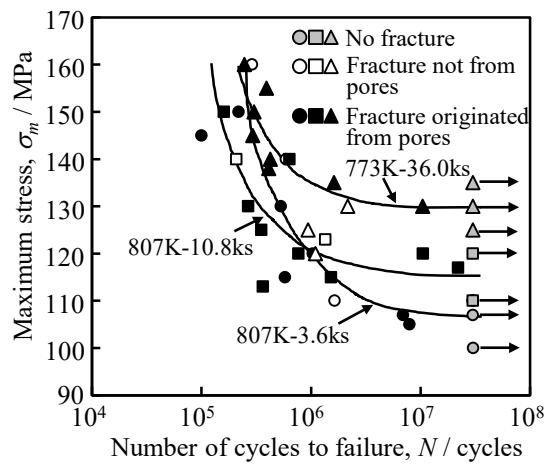
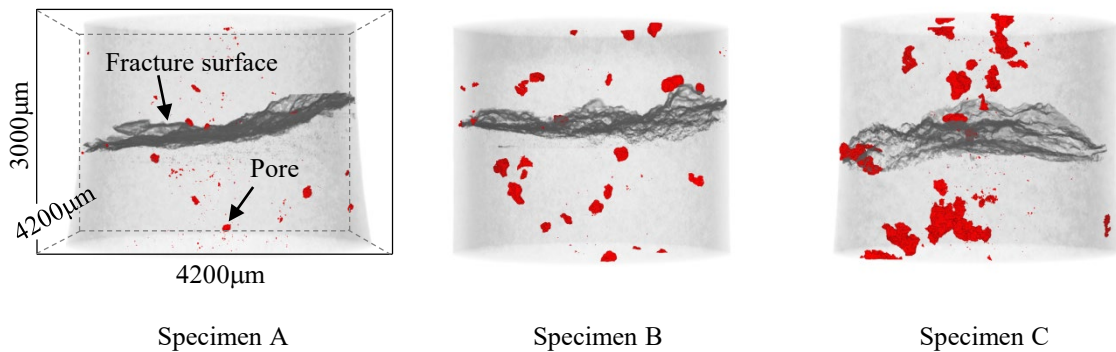
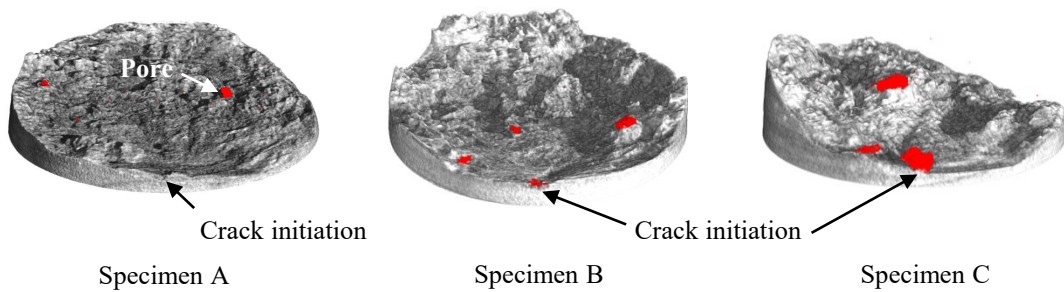


Fig.8 Classification of the data points shown in the S-N plots of Fig.6 according to the fracture originated from pores near specimen surface.

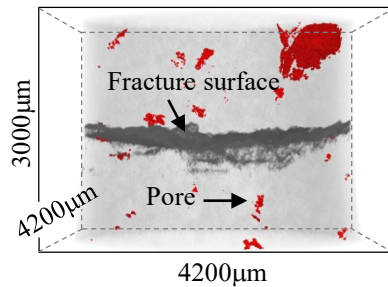


(a) 3D views of pores in the specimens that have been obtained by superposing 3D images captured before and after the fatigue tests.

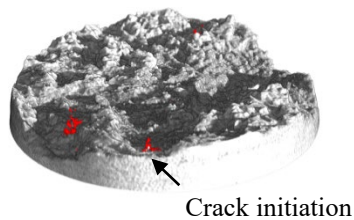


(b) 3D views of the fatigue fracture surface together with pores that caused fatigue fracture.

Fig.9 3D rendered perspective views of tomographic data, representing the spatial relationships between fracture surface and pores that had been solution-treated at 773K for 36.0ks. Specimen A: $V_f = 0.019\%$, $\sigma_m = 130$ MPa, $N = 2.2 \times 10^6$ cycles. Specimen B: $V_f = 0.111\%$, $\sigma_m = 145$ MPa, $N = 2.9 \times 10^5$ cycles. Specimen C: $V_f = 0.322\%$, $\sigma_m = 140$ MPa and $N = 4.2 \times 10^5$ cycles.



(a) 3D view of pores in a specimen that has been obtained by superposing 3D images captured before and after the fatigue test.



(b) 3D views of the fatigue fracture surface together with pores that caused fatigue fracture.

Fig.10 3D rendered perspective views of tomographic data, representing the spatial relationships between fracture surface and pores that had been solution-treated at 807K for 3.6ks. $V_f = 0.397\%$, $\sigma_m = 145\text{ MPa}$ and $N = 1.0 \times 10^5$ cycles.